

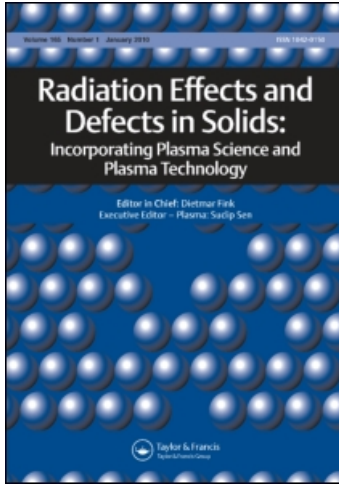
This article was downloaded by: [Inst Ciencias Nucleares]

On: 12 February 2010

Access details: Access Details: [subscription number 908761237]

Publisher Taylor & Francis

Informa Ltd Registered in England and Wales Registered Number: 1072954 Registered office: Mortimer House, 37-41 Mortimer Street, London W1T 3JH, UK



Radiation Effects and Defects in Solids

Publication details, including instructions for authors and subscription information:

<http://www.informaworld.com/smpp/title~content=t713648881>

Local modeling of collisionless magnetic reconnection in the dayside magnetosphere

Julio J. Martinell ^a

^a Instituto de Ciencias Nucleares, Universidad Nacional Autónoma de México, Mexico D.F., Mexico

Online publication date: 12 February 2010

To cite this Article Martinell, Julio J.(2010) 'Local modeling of collisionless magnetic reconnection in the dayside magnetosphere', Radiation Effects and Defects in Solids, 165: 2, 114 – 122

To link to this Article: DOI: 10.1080/10420150903516569

URL: <http://dx.doi.org/10.1080/10420150903516569>

PLEASE SCROLL DOWN FOR ARTICLE

Full terms and conditions of use: <http://www.informaworld.com/terms-and-conditions-of-access.pdf>

This article may be used for research, teaching and private study purposes. Any substantial or systematic reproduction, re-distribution, re-selling, loan or sub-licensing, systematic supply or distribution in any form to anyone is expressly forbidden.

The publisher does not give any warranty express or implied or make any representation that the contents will be complete or accurate or up to date. The accuracy of any instructions, formulae and drug doses should be independently verified with primary sources. The publisher shall not be liable for any loss, actions, claims, proceedings, demand or costs or damages whatsoever or howsoever caused arising directly or indirectly in connection with or arising out of the use of this material.

Local modeling of collisionless magnetic reconnection in the dayside magnetosphere

Julio J. Martinell*

*Instituto de Ciencias Nucleares, Universidad Nacional Autónoma de México,
A. Postal 70-543, Mexico D.F., Mexico*

Driven magnetic reconnection in the magnetospheric plasma, where collisions are extremely rare, is studied using a two-fluid collisionless plasma model. A local approximation is used for the dayside magnetosphere in which the magnetic field at the magnetopause has a null X -point with a guide field. Numerical computations are made for two situations that can occur: namely, a continuous solar wind drive and a bursty drive. They are compared under different circumstances focussing on the way the reconnection rate changes in time and on the resulting magnetic configurations. It is shown that the case of sequential impulsive events is more efficient than the continuous reconnection case.

Keywords: magnetosphere physics; magnetic reconnection; collisionless plasmas; numerical modeling; auroras

1. Introduction

The interaction of the solar wind magnetic field with the Earth's magnetosphere gives rise to various important phenomena such as geomagnetic substorms or flux transfer events (FTEs). It is now accepted that the physical process behind most of these episodes is magnetic reconnection, which takes place at different locations. Magnetic reconnection can occur either at the dayside of the magnetosphere or within the geomagnetic tail, and each one is associated with different observational phenomena. One result of reconnection is the conversion of magnetic energy into energetic particles, which move polewards along magnetic field lines giving rise to the aurora. It is believed that these events originate mainly at the geomagnetic tail, but it has been shown that dayside reconnection can also be important in producing auroral events. The latter can occur for both orientations of the solar wind magnetic field direction; for southward direction, the reconnection takes place near the equator, while high-latitude reconnection occurs for northward interplanetary magnetic field (IMF) directions in the solar wind. It has been found that high-latitude reconnection produces the so-called dayside proton auroral spots (I).

There is also the question of the duration of reconnection events. It is well known that the magnetic substorms are burst-like events that last for a short time, and the auroras also have a finite duration. On the other hand, the global dynamics of the magnetosphere indicates that magnetic reconnection occurs at a steady pace. It follows a cycle that starts with the creation of open field

*Email: martinell@nucleares.unam.mx

lines by dayside reconnection, which are convected by the solar wind to the nightside where they pile up along the magnetotail and then there appear closed field lines by the tail reconnection which convect back to the dayside. This cycle may occur through a continuous reconnection process that takes place at both places, the dayside and the magnetotail, simultaneously, but it might also result as a sequence of bursty reconnecting events. There is some controversy as to the nature of this process. At the geomagnetic tail, it is likely that reconnection is produced by high-speed regions of the solar wind, which increase the plasma pressure around the tail, and these are impulsive processes. On the dayside, there are non-steady processes such as FTEs (2) that involve merging of magnetic flux tubes, but due to a continuous flow of the solar wind, the reconnection can also happen steadily at certain places; its onset and ending would just depend on the direction of the IMF. However, owing to the changing conditions of the solar wind, some observations show a bursty sequence of reconnections (3), while others support the existence of a continuous process (4).

Here, we consider a dayside magnetic reconnection in the magnetopause. For low-latitude reconnection, the IMF is southward and there is evidence that favors intermittent behavior. In contrast, for northward IMF, there is high-latitude magnetic reconnection, which gives rise to dayside proton aurora and detailed observations show that it appears in a continuous way (4). The place of the reconnection moves about in longitude as the east–west direction of the IMF fluctuates, since the reconnecting field lines have to be always antiparallel, but the process does not stop. It is thus of interest to consider both steady and bursty magnetic reconnection events.

In general, the magnetic field does not have to be antiparallel for the reconnection to take place; it is possible to have a component of the magnetic field perpendicular to the plane of reconnection. This would correspond, for instance, to an east–west component of the IMF when the Earth's magnetic field is north–south, like in the noon position. This perpendicular field component (or guide field) is taken into account in the model presented here.

Magnetic line merging is initiated when two plasma regions having magnetic fields of opposite polarities are pushed together in what is known as driven reconnection. Since magnetospheric as well as solar wind plasmas are effectively collisionless, the mechanism for current limitation that leads to reconnection has to come from non-ideal effects such as electron inertia. Other effects, such as the Hall term in the generalized Ohm's law, may also contribute to the phenomenology. Many studies on collisionless magnetic reconnection have been made that include various terms in Ohm's law, with and without a neutral sheet, but few are directly applicable to the magnetospheric conditions.

For the parameters at the magnetosphere, $n \sim 10^{10} \text{ cm}^{-3}$, $T \sim 6 \text{ eV}$, $B \sim 10^{-4} \text{ G}$, the ion-sound gyroradius is $\rho_s \sim 20 \text{ km}$ while electron inertial skin depth is $d_e \sim 1 \text{ km}$. Additionally, for these parameters, one finds that the ratio of thermal to magnetic pressure is $\beta \sim 1/4$, so that the relevant regime to consider has $\rho_s > d_e$ but $\beta < 1$. Moreover, it is appropriate to model the local magnetic geometry by an X -point with a guide field normal to it. This would represent the meeting point of the solar wind IMF with the magnetosphere at the magnetopause, since the two fields would in general meet with directions having different angles relative to the ecliptic. This is one of the most studied configurations for driven magnetic reconnection: in this case, the drive provided by the convection of the solar wind plasma. A recent study of this geometry within the range $\rho_s/d_e > 1$ of current interest was presented in (5), but for the parameters relevant for the Versatile Toroidal Facility where reconnection experiments are conducted, including an approximate analytical estimate of the growth rate, as well as a numerical evaluation, but in the linear regime for the drive strength. A more complete analysis of collisionless driven reconnection has been addressed in (6), but the regime $\rho_s > d_e$ was not studied. Therefore, analyzed here is the evolution of an X -point configuration for the regime $\rho_s > d_e$ and in the presence of a guide field, for a compressible collisionless plasma taking into account the Hall effect. Full nonlinear

equations are used, as opposed to the works of (5, 6), where the linearized equations were analyzed analytically and numerically.

2. Driven reconnection model

The mathematical model used is based on the two-fluid equations with the quasi-neutrality condition $n_e = n_i = n$. The relevant equations are the particle conservation equation and the ion momentum and electron momentum equations:

$$\frac{\partial n}{\partial t} = -\nabla \cdot (n \mathbf{V}_i), \quad (1)$$

$$m_i \left[\frac{\partial}{\partial t} + (\mathbf{V}_i \cdot \nabla) \right] \mathbf{V}_i = e \mathbf{E} + \frac{e}{c} \mathbf{V}_i \times \mathbf{B} - e \eta \mathbf{J}, \quad (2)$$

$$\mathbf{E} + \frac{1}{c} \mathbf{V}_e \times \mathbf{B} = -\frac{m_e}{e} \left[\frac{\partial}{\partial t} + (\mathbf{V}_e \cdot \nabla) \right] \mathbf{V}_e + \eta \mathbf{J} - \frac{\nabla p}{en}, \quad (3)$$

where the current is $\mathbf{J} = ne(\mathbf{V}_i - \mathbf{V}_e)$ and the fields are governed by Maxwell's equations without the displacement current. The ions are assumed to be cold. All quantities have their usual meanings. Although this paper is interested in a collisionless plasma, the resistivity η is included here for completeness and for comparison purposes, but will eventually be made zero.

A Cartesian geometry is considered, symmetric along the z coordinate, having an equilibrium X -point magnetic configuration in the (x, y) -plane and a guide field in the z -direction. The magnetic field is represented by $\mathbf{B} = \hat{z} \times \nabla \psi(x, y, t) + B_z(x, y, t) \hat{z}$. The equilibrium magnetic potential that gives an hyperbolic X -point is $\psi_0 = B'_\perp x y$ and is characterized by a scale length defined by $l_0 \equiv B_{z0}/B'_\perp$. The ion velocity is actually the plasma velocity $\mathbf{V}_i = \mathbf{v}$, and a general representation can be given in terms of the potentials ϕ and χ (related to the plasma compressibility) as $\mathbf{v}_i = \hat{z} \times \nabla \phi(x, y, t) + \nabla \chi(x, y, t) + v_z(x, y, t) \hat{z}$. In the equilibrium state, the values $\mathbf{v}_0 = 0$, $\mathbf{J}_0 = 0$ and $n_0 = \text{constant}$ are taken. Then, the two-fluid equations are taken for the strong guide field orderings, $\beta < 1$ and $l_0/d_i \gg 1$, where $d_i = c/\omega_{pi}$ is the ion skin depth. In the limit $v_z \rightarrow \infty$, they can be reduced to a set of three equations for the three perturbed variables ψ , ϕ and the density n , which enters through the variable $\xi \equiv (l_0/d_i) \log(n/n_0)$. They follow from the component $\hat{z} \cdot \nabla \times$ of Equation (2) and the component $\hat{z} \cdot$ of Equation (3). These equations are (7):

$$\frac{\partial U}{\partial t} = [U, \phi] + [\psi, \nabla^2 \psi], \quad (4)$$

$$\frac{\partial}{\partial t} (\psi - d_e^2 \nabla^2 \psi) = [\psi - d_e^2 \nabla^2 \psi, \phi] - \rho_s^2 [\psi, \xi] + \epsilon_\eta \nabla^2 \psi, \quad (5)$$

$$\frac{\partial \xi}{\partial t} = [\xi, \phi] + [\psi, \nabla^2 \psi], \quad (6)$$

where $[f, g] \equiv \hat{z} \cdot \nabla f \times \nabla g$, $U \equiv \nabla^2 \phi$ is the vorticity and all variables are normalized according to $\phi \rightarrow \phi/(l^2/\tau_A)$, $\psi \rightarrow \psi/(l^2 B'_\perp)$, the lengths to the system size l and the time to the Alfvén time $\tau_A = (4\pi n_0 m_i)^{1/2}/B'_\perp$. The term proportional to ρ_s in Equation (5) is proportional to the electron compressibility and the resistive term is given by $\epsilon_\eta = (d_e/l)^2 \nu_{ei} \tau$, with ν_{ei} the electron-ion collision frequency.

A linearized version of this set of equations was studied in (5, 6), for the case of forced reconnection by an induced electric field in an X -point, finding time-asymptotic analytical solutions that were corroborated numerically. A nonlinear simulation of a similar model was made in (8) but for an initial equilibrium of the type of a neutral current sheet and for parameters not relevant

to the magnetosphere. Equations (4)–(6) can be simplified to the so-called reduced model for reconnection when $U = \xi$. This model, as well as other models, has been studied by Aydemir (9) in driven X -point reconnection, and he showed that the reconnection rate is independent of the particular model, being determined only by the external driving features, which are introduced through the boundaries. A similar conclusion can be reached for the current model, as will be shown below.

When the external drive leading to reconnection is weak, the linearized equations can be simplified to a single equation which can be solved analytically in the time-asymptotic limit (5), but the full-time evolution has to be obtained numerically. In order to study the nonlinear evolution of the X -point configuration, Equations (4)–(6) are solved numerically, starting from the equilibrium state mentioned above and driving an inwards flow from the boundaries of the domain considered. The numerical method used is based on a finite difference leapfrog trapezoidal scheme in a finite square box of size L . The imposed flow at the boundary with a velocity v_0 is given in terms of the stream function by

$$\phi(x, y, t = 0) = \frac{v_0 l_0}{4} \ln \left(\frac{y^2 + \delta^2}{x^2 + \delta^2} \right), \quad (7)$$

where δ is a parameter used to avoid singularities and is of order ρ_s . The boundary conditions are applied at $(x, y) = \pm L$ and $L = 1$ is taken. For ϕ , ξ and U , the boundary values of the functions are fixed to their equilibrium values plus a driving function, while for ψ and J , the values of the normal derivatives are the ones specified. The time-dependent boundary conditions are in accordance with Equation (7):

$$\phi(\pm 1, y, t) = \frac{1}{4B'_\perp} f(t) \ln(y^2 + \delta^2), \quad \phi(x, \pm 1, t) = -\frac{1}{4B'_\perp} f(t) \ln(x^2 + \delta^2), \quad (8)$$

$$\frac{\partial \psi(\pm 1, y, t)}{\partial y} = B'_\perp y, \quad \frac{\partial \psi(x, \pm 1, t)}{\partial x} = B'_\perp x, \quad (9)$$

and $\xi(\pm 1, y, t) = \xi(x, \pm 1, t) = 0$, where $f(t)$ is the time-dependent driving function. For an impulsive drive,

$$f(t) = v_0 B_{z0} \left(\frac{t}{\tau_d} \right) \exp \left[\frac{-t}{\tau_d} \right], \quad (10)$$

is used, while for a steady forcing:

$$f(t) = v_0 B_{z0} \left(1 - \exp \left[\frac{-t}{\tau_d} \right] \right). \quad (11)$$

These expressions are chosen in such a way as to start at zero for $t = 0$ and then have a growth with a characteristic time τ_d . The initial conditions inside the computational domain are $\phi(x, y, t = 0) = 0$, $\xi(x, y, t = 0) = 0$ and $\psi(x, y, t = 0) = B'_\perp xy$.

The numerical code was benchmarked for a case of low and continuous forcing with $V_I = v_0 l_0 = 0.1$ and it was found that the system evolves to reach a steady reconnection state which corresponds to the asymptotic analytical solution found in (5) for the central current density. The parameters used over most studies were $\rho_s^2 = 0.2$, $d_c^2 = 0.02$, $l_0/d_i = 2$. The guide field magnitude is included in l_0 . The cases with no guide field are not described by these equations and thus they will not be addressed here. In the following, the numerical computations for the three relevant quantities ξ , ϕ and ψ , as well as the vorticity U and current density $J = \nabla^2 \psi$ are shown. In most of the results presented, the collisionless limit is taken, with $\epsilon_\eta = 0$, and the resistivity is just taken into account for comparative cases, which are explicitly mentioned.

3. Impulsive and continuous reconnection

We assume that some perturbation in the solar wind is pushing on the external boundary of our simulation region and thus the time evolution starts when a velocity drive is produced as a boundary condition in the initial equilibrium state $\psi_0 = B'_\perp xy$. We first use the continuous drive given by Equation (10) in the boundary condition (Equation (8)). The important parameter in determining the reconnection properties is the driving strength V_I . As it was found in (9), it can be obtained that for low V_I the X -point maintains its configuration as reconnection proceeds and thus the induced current is concentrated mainly around the X -point. However, for large V_I , the strong forcing is faster than the reconnection rate and the X -point flattens to form a current sheet. This indicates that the external conditions, imposed through the boundaries, are the main factors in determining the reconnection properties, as concluded in (9). Here, the resistive case is used as a reference to compare the collisionless results. In that case, the reconnection starts increasing during the drive characteristic time, which is taken as $\tau_d = 1.0$, and then the magnetic flux grows at a steady pace, giving a constant reconnection rate γ_{R0} . Similarly, the current grows in a time of a few τ_{dS} and then it saturates at a constant value J_m . This behavior is obtained for all values of the driving strength V_I . It is found that both γ_{R0} and J_m increase with B'_\perp and V_I with almost linear dependence. In fact, the following relations hold true

$$\frac{\gamma_{R0}}{B'_\perp} \sim V_I^\alpha, \quad \frac{J_m}{B'_\perp} \sim V_I^\alpha, \quad (12)$$

with $\alpha \geq 1$.

Figure 1 shows the final configurations for the velocity potential ϕ , the magnetic potential or magnetic flux ψ , the density ξ and the current J , after the transient time has elapsed, for both the resistive and the collisionless cases. The diagrams represent constant contour plots of the respective quantities and thus they give the velocity stream lines (ϕ) and the magnetic field lines (ψ). The flow is incoming from the lower-left and upper-right corners and exits from the lower-right and upper-left corners. At earlier times, U and ξ evolve independently but at this late stage it is found that the vorticity coincides with the density, *i.e.* $U = \xi$, which is precisely the condition for the reduced model to apply. This means that the system tends to adjust itself to that model and

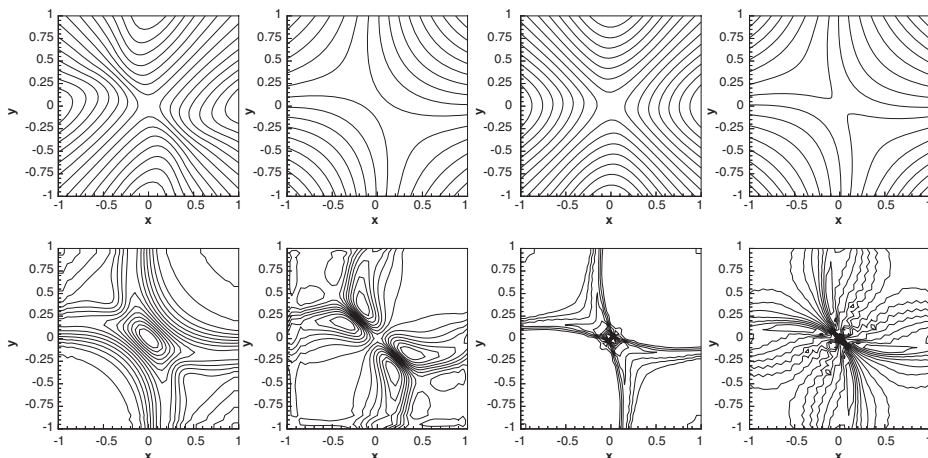


Figure 1. Contour plots for ϕ and ψ (upper row) and current J and density ξ (lower row). The resistive case is on the left-hand side and the collisionless case on the right-hand side. For both cases, $B'_\perp = 0.6$, $V_I = 0.4$, and for the resistive case, $\epsilon_\eta = 0.1$, while $d_c^2 = 0.02$ and $\rho_s^2 = 0.2$ for the collisionless case.

then Equations (6) and (4) give the same evolution, reducing the system to just two Equations ((4) and (5)) that have been studied repeatedly. The high driving strength with $V_I = 0.4$ is used here, which is enough to produce a current sheet in both cases. The formation of a noticeable current sheet occurs for $V_I \geq 0.1$. For the collisionless case, the current sheet becomes unstable for the strong drive and the smooth structure is destroyed, so the times shown for that case correspond to earlier times than for the resistive case.

The central value of ψ gives a measure of the reconnected magnetic flux, and the reconnection rate will be defined by $\gamma_R = d\psi(r=0)/dt$. In Figure 2, the time evolution of $\psi(r=0) = \psi_0$ is shown, together with that of the central current density, $J(r=0)$, for a moderate drive of $V_I = 0.1$. The slope of the curve $\psi_0(t)$ gives γ_R . For comparison, also shown is the reconnected flux ψ_0 and J_m for the purely resistive case. They are given by the dashed curves which correspond to $\epsilon_\eta = 0.1$ and $\rho_s = d_e = 0$. It is clear that in this case, both γ_R and $J(0)$ approach a constant value, which is determined solely by the forcing strength, as given by Equation (12). However, for the collisionless case, the growth rate and current are continuously changing and there is no tendency of getting to an asymptotic limit. In contrast, the low forcing case behaves more like the resistive case, reaching constant values for γ_R and J_m . As can be seen, the collisionless reconnection proceeds initially at a slower rate than the resistive one, since the noncollisional effects that lead to reconnection are weaker, but as time increases γ_R grows substantially and then goes back to a moderate value but still about 50% larger than the resistive one for the parameters of Figure 2. The high γ_R is associated with a large current rise too, leading to very large final values of J_0 , but very localized at the X -point position.

The second case studied is the impulsive drive. This is given by Equation (11), which lasts only a time of the order τ_d . It is expected that the reconnection will only last a finite time, as the drive is pulsed. That could be the result of a solar wind gust buffeting the magnetosphere, which would lead to short-lived reconnection and it will die out at large times. That is indeed the situation found, with the physical features obtained for continuous forcing remaining almost the same, during the reconnection period. However, the important issue is the decaying time of the reconnection process once the drive is over. As it turns out, the plasma near the X -point takes quite a long time to go back to its original state, especially when the drive is strong. In Figure 3,

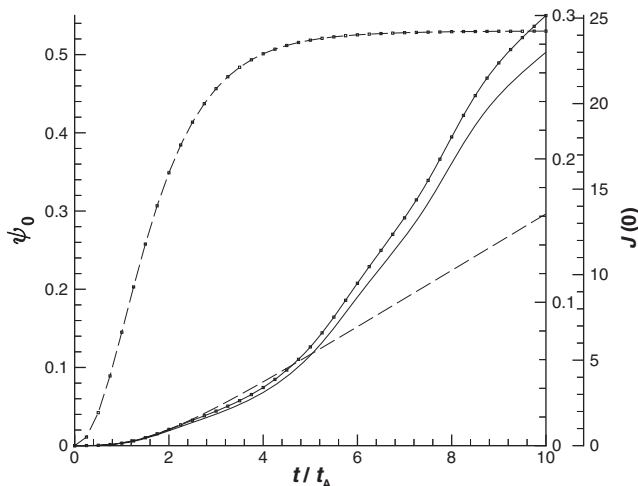


Figure 2. Reconnected magnetic flux ψ_0 and X -point current $J(0)$ as functions of time with continuous drive for the resistive case (dashed lines) and collisionless plasma (solid lines). Curves for $J(0)$ are marked with circle symbols and correspond to scales at the right axes. The larger scale (0–25) is for the collisionless case, while the resistive case has lower currents (0–0.3).

the time evolution of ψ_0 and J is depicted for a collisionless plasma when the forcing is moderate ($V_1 = 0.1$). The development of the instability observed for continuous forcing is still playing a role, since the current does not fall back to zero immediately after the flux stops growing. The growth rate γ_R is essentially zero after a time $t \approx 4\tau_d = 1$, while the current remains at $J(0) \approx 1$ for several times τ_d .

This will have important consequences when there are multiple impulses in a sequence, since the remaining effects of the first pulse will affect the initial conditions for the second pulse and so on. This will be relevant in the magnetosphere when consecutive solar ejections (coronal mass ejections) or similar events arrive at the magnetosphere. The resulting reconnecting events will

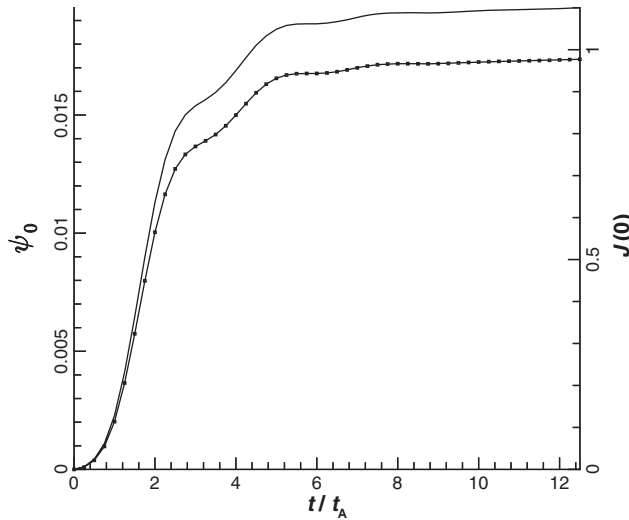


Figure 3. Reconnected magnetic flux ψ_0 and X-point current $J(0)$ as functions of time for the collisionless case with an impulsive drive with a time constant, $\tau_d = 1$. The curve marked with circle symbols refers to $J(0)$ with its scale on the right-hand side axis.

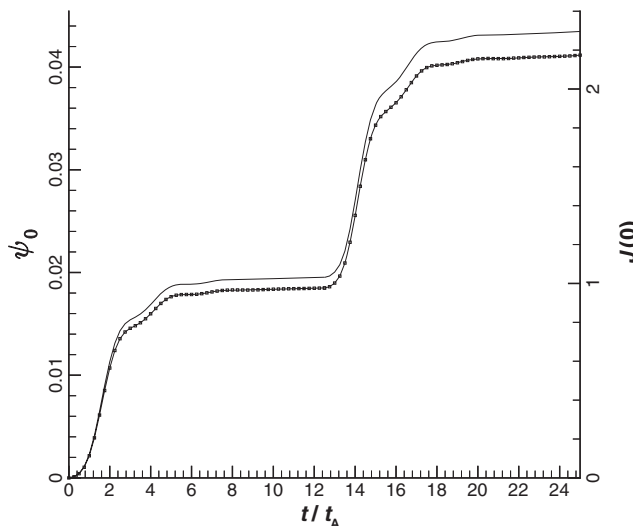


Figure 4. Time evolution of the reconnected magnetic flux ψ_0 and X-point current $J(0)$ for the case of two pulses applied in sequence separated in time $12.5\tau_d$, with $\tau_d = 1$. Notice the same evolution for $J(0)$ (marked with circle symbols) and ψ_0 .

have a memory of the previous pulses and the magnetic configurations would be different. Such an example is shown in Figure 4, which represents the evolution of ψ_0 and $J(0)$ upon the arrival of two pulses separated in time $T = 12\tau_d$. Naturally, the amount of reconnected flux increases with the arrival of each pulse, but the central current also keeps increasing when the pulses arrive in sequence. Thus, in some sense, these processes act as some kind of continuous reconnection, keeping track of the previous events. Only if the separation between pulses is very long, the plasma will return to its initial state after the reconnection and one will have the effect of independent impulsive events.

4. Conclusions

This paper has studied the magnetic reconnection phenomenon in a collisionless plasma having the physical conditions relevant to the magnetosphere, *i.e.* $\rho_s > d_e$ and $\beta < 1$. The issue of having continuous drive or a pulsed drive was addressed, since this is of great relevance in the dayside magnetosphere. As a representative local magnetic configuration, we used an X -point geometry which initially is in equilibrium with zero electrical current. The mathematical model consists of three equations for the three fields ϕ , ψ and the density. It was shown that this model converges to the reduced model with only two equations, in the time-asymptotic situation.

For the case of a continuous forcing, some differences were found between the current model and the resistive model, dominated by collisions. When compared with the resistive case, the collisionless model has an initially slower reconnection rate, but after a few Alfvén times, it starts growing faster so that there is a larger net reconnected flux in the case with no collisions. The spatial distributions are more compact in the sense that the currents are concentrated into smaller volumes. Then the case of impulsive drive showed that while ψ_0 approaches a final value after the drive has finished, the current is maintained without falling off for a longer time. This has the effect that when there are multiple pulses arriving in sequence to drive the reconnection, there is some degree of memory that continues to increase the total reconnected magnetic flux and the X -point current. This accumulative effect will act in the same way as the continuous drive.

These results may explain the observations reported in (4) of the continuous presence of auroral spots for periods of 4–9 h, which indicate a that continuous reconnection event was taking place, even for different solar wind conditions. They also showed evidence that the reconnection does not stop for periods longer than 5 min. This can be understood in terms of multiple pulses, since the final result is to give the appearance of a continuous reconnection, even when the drive is switching on and off. As Figure 4 shows, the magnetic flux and the X -point current are always increasing, although at a slow pace between pulses. For the parameters in the magnetosphere given in Section 1 and $l_0 = 10$ km, the Alfvén time is $\tau_A \approx 4 \times 10^3$ s, which means that the reconnection process for a single pulse continues for more than 1 h, explaining the timescales reported in (4).

Acknowledgement

This work was partially supported by the Conacyt project 81232 and DGAPA-UNAM project IN119408.

References

- (1) Frey, H.U.; Mende, S.B.; Immel, T.J.; Fuselier, S.A.; Clafin, E.S.; Gérard, J.-C.; Hubert, B. *J. Geophys. Res.* **2002**, *107* (A7), 1091–1–17.
- (2) Russell, C.T.; Elphic, R.C. *Geophys. Res. Lett.* **1979**, *6*, 33–36.
- (3) Milan, S.E.; Lester, M.; Greenwald, R.A.; Sofko, G. *Ann. Geophys.* **1999**, *17*, 1166–1171.

- (4) Frey, H.U.; Phan, D.T.; Fuselier, S.A.; Mende, S.B. *Nature* **2003**, *426*, 533–537.
- (5) Ramos, J.J.; Porcelli, F.; Verastegui, R. *Phys. Rev. Lett.* **2002**, *89*, 055002-1–4.
- (6) Delzanno, G.L.; Fable, E.; Porcelli, F. *Phys. Plasmas* **2004**, *11*, 5212–5228.
- (7) Kuvshinov, B.N.; Lakhin, V.P.; Pegoraro, F.; Schep, T.J. *J. Plasma Phys.* **1998**, *59*, 727–736.
- (8) Fitzpatrick, R. *Phys. Plasmas* **2004**, *11*, 937–946.
- (9) Aydemir, A.Y. *Phys. Plasmas* **2005**, *12*, 080706-1–4.